IOP Publishing | The Japan Society of Fluid Mechanics Fluid *Dynamics* Research

Fluid Dyn. Res. **46** (2014) 061424 (15pp) doi:10.1088/0169-5983/46/6/061424

Towards a theory for vortex filaments in stratified-rotating fluids

Paul Billant[1], Axel Deloncle[1], Jean-Marc Chomaz[1] and Pantxika Otheguy[1,2]

[1] LadHyX, CNRS, Ecole Polytechnique, F-91128 Palaiseau Cedex, France
[2] Centre Technique Littoral, Lyonnaise des Eaux, Pavillon Izarbel, 64210 Bidart, France

E-mail: billant@ladhyx.polytechnique.fr

Received 31 January 2014, revised 18 October 2014
Accepted for publication 21 October 2014
Published 25 November 2014

Communicated by Y Hattori

Abstract

In inviscid fluids with uniform density, it is common to idealize three-dimensional vortex tubes by filaments (i.e., single lines of an infinitesimal cross section). Thanks to the Kelvin and Helmholtz theorems, it is known that these vortex filaments are transported with the fluid and their circulation is conserved. The induced motions can be computed by the Biot–Savart law, with an appropriate cut off in the integral to avoid singularity. Hence, this approach allows one to model the linear or nonlinear dynamics of vortex flows. *A priori*, vortex filaments cannot be used in density-stratified and rotating fluids since the circulation is not conserved and the vortex lines are not material lines. However, in this paper we review a theory that is equivalent to vortex filaments. It is based on matched asymptotic expansions for small vortex-core size, weak curvature, and small vortex displacements. The resulting stability equations are formally identical to those of vortex filaments in homogeneous fluids. However, striking differences between homogeneous and stratified-rotating fluids exist, such as the reversal of the self-induced motion for strong stratification or complex self-induction for moderate stratification due to the presence of critical points. The three-dimensional linear stability of vertical vortex pairs and vortex arrays (Karman street, double symmetric row) in stratified and rotating fluids has been investigated using this analytical approach. The results are in very good agreement with the results of direct numerical stability analyses of smooth vortex configurations. Possible extensions to include nonlinear and baroclinic effects are briefly discussed.

(Some figures may appear in colour only in the online journal)

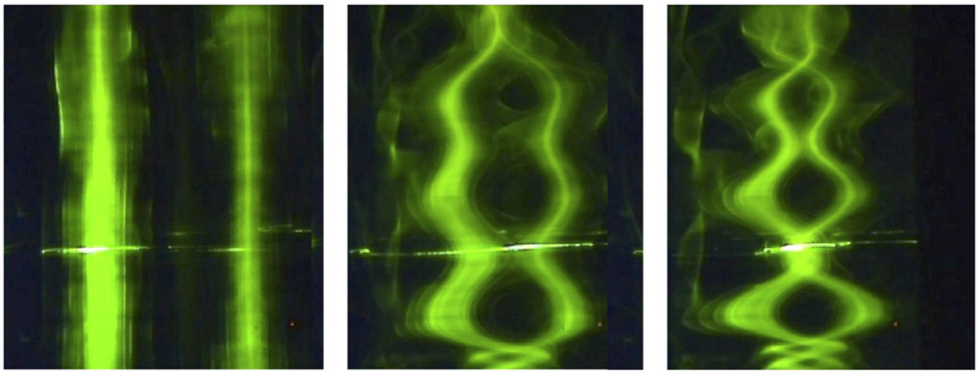

Figure 1. Visualizations of the zigzag instability of two co-rotating vortices in a strongly stratified fluid. The vortices are created by two facing vertical plates rotating in opposite directions. The flow is visualized by fluorescein dye released at the edges of the plates and illuminated by ultraviolet light. The images have been taken at $t = 0$ s, $t = 81$ s and $t = 87$ s (Otheguy 2005).

1. Introduction

The dynamics and behaviour of vortices are fundamentally different in stratified-rotating fluids and homogeneous fluids. In particular, three-dimensional instabilities of vortices strongly depend on stratification and/or background rotation. The elliptic instability for an unbounded, strained vertical vortex is inhibited as soon as the buoyancy frequency, N, is larger than the angular velocity of the vortex (Miyazaki and Fukumoto 1992, Miyazaki 1993, Kerswell 2002, Leblanc 2003). In contrast, the Rayleigh criterion for the centrifugal instability in inviscid fluids is independent of stratification and depends only on background rotation (Kloosterziel and van Heijst 1991, Billant and Gallaire 2005).

It has also been shown that co- and counter-rotating vertical vortex pairs in strongly stratified fluids are unstable to a long-wavelength bending instability called zigzag instability, which is shown in figure 1 (Billant and Chomaz 2000, Otheguy *et al* 2006). Such instability bends the vortices with almost no internal deformation of the vortex cores, in contrast to the elliptic instability. It leads to a layered structure, as is often observed in strongly stratified flows (Riley and Lelong 2000). Similar bending instabilities have been reported in quasi-geostrophic flows (Dritschel and de la Torre Juárez 1996). In homogeneous fluids, counter-rotating vortex pairs are also subject to a long-wavelength bending instability known as the Crow instability (Crow 1970), which is symmetric, in contrast to the zigzag instability which is antisymmetric.

In the case of co-rotating vortex pairs, stability analyses (Otheguy *et al* 2006) have shown that the zigzag instability is dominant when the stratification is strong. Its growth rate is constant and proportional to the strain, $\Gamma/(2\pi b^2)$, when the Froude number, $F_h = \Gamma/(2\pi R^2 N)$, is below unity, where Γ is the circulation, R is the vortex radius, and b is the separation distance between the two vortices. When the Froude number is larger than unity, the growth rate of the zigzag instability drops abruptly and goes to zero for $F_h \simeq 1.8$ in the case of a nonrotating fluid. Above this critical Froude number, and in particular in homogeneous fluids, co-rotating vortex pairs are stable to long-wavelength bending perturbations (Jiménez 1975). In the presence of a background rotation (Otheguy *et al* 2006), the zigzag instability remains dominant when the stratification is strong. Its growth rate scales

like the strain, independently of the Rossby number, $Ro = \Gamma/(4\pi R^2\Omega_b)$, where Ω_b is the rate of background rotation around the vertical axis.

In homogeneous fluids, the Crow instability has been described by means of vortex filaments and the Biot–Savart law. This method cannot be applied in stratified-rotating fluids because the circulation is not conserved. However, an analogous analysis can be carried out via matched asymptotic expansions by assuming well-separated vortices and small long-wavelength bending deformations of the vortices (Billant 2010, Billant *et al* 2010, Deloncle *et al* 2011). In this paper, we review and summarize the main steps of this asymptotic approach and its results, and we emphasize the physical mechanism of the bending instabilities. Possible extensions to include nonlinear and baroclinic effects are also briefly discussed in the conclusion.

2. Theoretical description of bending instabilities

To determine how we can theoretically describe bending instabilities in a stratified-rotating fluid, it is interesting to first look at the same problem in homogeneous and non-rotating fluids as first considered by Crow (1970).

2.1. Homogeneous fluids

To describe the symmetric bending instability of counter-rotating vortex pairs in homogeneous fluids, Crow (1970) idealized the two vortices by two singular lines of vorticity (i.e., two vortex filaments). Owing to the Kelvin and Helmholtz theorems, their circulation, Γ, is conserved and they are advected like material lines in inviscid fluids. Hence, the Biot–Savart law reduces to

$$\boldsymbol{u}(\boldsymbol{x}) = -\frac{\Gamma}{4\pi}\int \frac{(\boldsymbol{x}-\boldsymbol{x}')\times \mathrm{d}\boldsymbol{l}(\boldsymbol{x}')}{|\boldsymbol{x}-\boldsymbol{x}'|^3}, \tag{1}$$

where $\mathrm{d}\boldsymbol{l}(\boldsymbol{x}')$ is a vortex element. The velocity, $\boldsymbol{u}(\boldsymbol{x})$, induced by a vortex filament can be computed at any point by knowing only the position of the filament. A problem of this method is that (1) diverges logarithmically if the filament is curved when computing the self-induced velocity (i.e., when $\boldsymbol{x}$ approaches $\boldsymbol{x}'$). One can avoid this divergence by integrating the Biot–Savart law over all of the vortex except a small segment, d, on either side of the point where the velocity is evaluated. This cut-off method amounts to taking into account the finite size of the vortex cores (Crow 1970, Saffman 1992). It gives

$$\boldsymbol{u}(\boldsymbol{x}) = -\frac{\Gamma}{4\pi}\int_{|\boldsymbol{x}-\boldsymbol{x}'|>d} \frac{(\boldsymbol{x}-\boldsymbol{x}')\times \mathrm{d}\boldsymbol{l}(\boldsymbol{x}')}{|\boldsymbol{x}-\boldsymbol{x}'|^3} = -\frac{\Gamma}{4\pi\rho}\boldsymbol{b}\left(\ln\frac{d}{\rho}+O(1)\right), \tag{2}$$

where ρ is the local radius of curvature and $\boldsymbol{b}$ is the unit vector in the binormal direction (see figure 3). This cut-off method has been rigorously justified by considering a slightly curved vortex with a finite radius, R (Widnall *et al* 1971, Moore and Saffman 1972, Leibovich *et al* 1986, Fukumoto and Miyazaki 1991). In this case, the structure of the vortex can be determined by means of matched asymptotic expansions with the small parameter, R/ρ. This yields an expression for d that is valid at the leading order in R/ρ:

$$d = \frac{R}{2}\exp\left(\frac{1}{2}-D\right), \tag{3}$$

with

$$D = \lim_{\eta_0 \to \infty} \int_0^{\eta_0} \xi^3 \Omega(\xi)^2 \mathrm{d}\xi - \ln \eta_0, \tag{4}$$

where Ω is the angular velocity nondimensionalized by $\Gamma/(2\pi R^2)$. Using this cut-off parameter, vortex filaments are the leading order approximation in R/ρ of a vortex with a gently bent finite core. By using this method, Crow (1970) was able to compute the interaction between two counter-rotating vortices in homogeneous fluids, and to show that they are unstable to a long-wavelength symmetric instability.

2.2. Stratified-rotating fluids

In the case of stably stratified-rotating inviscid fluids, the equations of momentum, continuity, and density conservation under the Boussinesq approximation are

$$\frac{\mathrm{D}\boldsymbol{u}}{\mathrm{D}t} + 2\Omega_b \boldsymbol{e}_z \times \boldsymbol{u} = -\frac{1}{\rho_0}\nabla p - \frac{g\rho'}{\rho_0}\boldsymbol{e}_z, \tag{5}$$

$$\nabla \cdot \boldsymbol{u} = 0, \tag{6}$$

$$\frac{\mathrm{D}\rho'}{\mathrm{D}t} + \frac{\partial \bar{\rho}}{\partial z} u_z = 0, \tag{7}$$

with $\boldsymbol{u} = (u_x, u_y, u_z)$ as the velocity in cartesian coordinates (x, y, z), Ω_b as the rotation rate about the vertical axis, $\boldsymbol{e}_z$ as the vertical unit vector, p as the pressure, g as the gravity, $\rho'(x, y, z, t)$ as the perturbation density relative to the sum of a constant reference density, ρ_0, and a mean density profile along the vertical $\bar{\rho}(z)$.

Because of the Coriolis and buoyancy forces in (5), the Kelvin and Helmholtz theorems are not valid; the circulation is not conserved and the vortex lines do not move like material lines. Nevertheless, Ertel's theorem states that the potential vorticity, $\Pi = (2\Omega_b \boldsymbol{e}_z + \boldsymbol{\omega}) \cdot \nabla(\bar{\rho}(z) + \rho')$, where $\boldsymbol{\omega} = \nabla \times \boldsymbol{u}$ is the vorticity, is conserved following the motion. This quantity is generally nonlinear in terms of the flow variables, so it cannot be easily inverted to obtain the velocity induced by a singular line of potential vorticity. An inversion is possible only in the quasi-geostrophic limit, since the potential vorticity and the streamfunction of the flow are then related by a linear operator relationship.

Hence, the vortex filament concept used in homogeneous fluids cannot be directly applied to stratified-rotating fluids. As an alternative, we can consider two vortices with circulation Γ_1 and Γ_2 with finite cores, perturbed by long-wavelentgh bending perturbations and separated by a large distance, b, compared to their radius, R (figure 2). These are the two hypotheses behind vortex filaments in homogeneous fluids. Using these hypotheses, the stability of the vortex pair can be computed asymptotically by means of the two small parameters:

$$\frac{R}{b} \ll 1, \qquad kR \ll 1, \tag{8}$$

where k is the vertical wavenumber of the perturbation.

A priori, such asymptotic analysis can be performed for any Froude and Rossby numbers based on the circulation of each vortex, $i = \{1, 2\}$

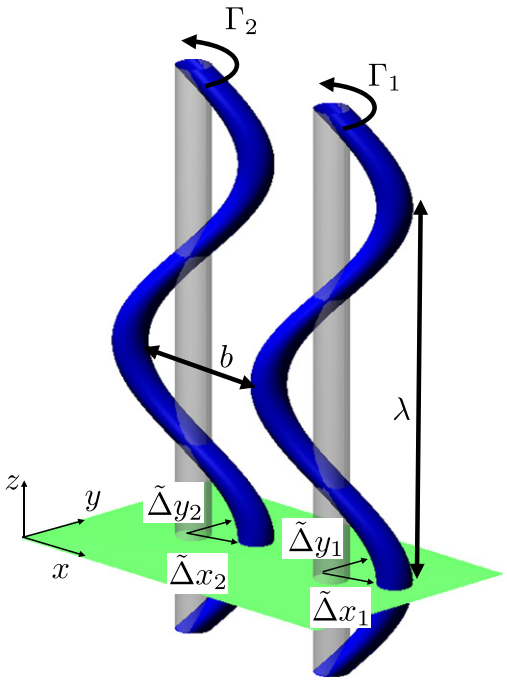

Figure 2. Sketch of the asymptotic problem. We consider two vertical vortices that are separated by a large distance, b, compared to their radius, R, and perturbed by long-wavelength bending deformations, $\lambda = 2\pi/k \gg R$, in a stratified-rotating fluid.

$$F_{hi} = \frac{|\Gamma_i|}{2\pi R^2 N}, \qquad Ro_i = \frac{\Gamma_i}{4\Omega_b \pi R^2}, \tag{9}$$

where $N = \sqrt{-(g/\rho_0)\partial\bar{\rho}/\partial z}$ is the Brunt–Väisälä frequency, which is assumed to be constant. However, a condition on the Froude number shows up in the course of the analysis (see (12)). Here, we will only summarize the main steps of this asymptotic analysis, which is performed in Billant (2010).

At the leading order in wavenumber kR and separation ratio R/b, equations (5)–(7), which are linearized around the base vortices, reduce to two-dimensional stability equations for each vortex, as if they were independent. The perturbation is chosen as small displacements $(\tilde{\Delta}x_i(z, t), \tilde{\Delta}y_i(z, t))$ of each vortex, $i = \{1, 2\}$. For example, the streamfunction of the perturbation at the leading order reads

$$\tilde{\psi}^{(0)} = -\tilde{\Delta}x_1 \frac{\partial \psi_1}{\partial x} - \tilde{\Delta}y_1 \frac{\partial \psi_1}{\partial y} - \tilde{\Delta}x_2 \frac{\partial \psi_2}{\partial x} - \tilde{\Delta}y_2 \frac{\partial \psi_2}{\partial y}, \tag{10}$$

where ψ_1 and ψ_2 are the streamfunction of each basic vortex. This solution is an exact solution, whatever the stratification and background rotation. It derives from the translational invariance, which implies that $\psi_1(x - \tilde{\Delta}x_1, y - \tilde{\Delta}y_1) + \psi_2(x - \tilde{\Delta}x_2, y - \tilde{\Delta}y_2)$ is a solution whatever the displacements, provided that the two vortices are far apart. These displacements can be written in the form $(\tilde{\Delta}x_i, \tilde{\Delta}y_i) = (\Delta x_i(t), \Delta y_i(t))e^{ikz} + \text{cc}$ where $i = \{1, 2\}$.

At the next order in kR and R/b, three-dimensional effects and interaction between displacement perturbations of each vortex show up in equations (5)–(7), linearized around the base vortices. These effects can interact if they are of the same order: $O(1/k) = O(b)$. To

solve the asymptotic problem, two regions need to be considered: a core region near each vortex where the radius $r = O(R)$, and a far-field region such that $r = O(1/k) = O(b)$. The second-order solution can be found analytically in the core region using (10) (see Billant 2010). In the outer region, since the angular velocity of the base vortices decays like $\Gamma_i/(2\pi r^2)$, the local Froude and Rossby numbers at a distance, b, from the vortex center are $F_{hb} = |\Gamma_i|/(2\pi N b^2)$ and $Ro_b = \Gamma_i/(4\pi\Omega_b b^2)$. Hence, if b is sufficiently large, the local Froude and Rossby numbers are small, meaning that the flow is quasi-geostrophic. Since the potential vorticity is initially constant outside the vortex cores, the potential vorticity of the perturbation is zero $\tilde{\Pi} = \Delta_h\tilde{\psi} - \beta^2\tilde{\psi} = 0$, where $\tilde{\psi}$ is the streamfunction of the perturbation and $\beta = 2k|\Omega_b|/N$. The streamfunction of the outer solution is therefore of the form

$$\tilde{\psi} = K_m(\beta r)\mathrm{e}^{\pm \mathrm{i}m\theta}, \tag{11}$$

where K_m is the modified Bessel function of the second kind of order m. This outer solution will be valid if the local Froude and Rossby numbers, F_{hb} and Ro_b, are small. In practice, it can be shown that only the local Froude number, F_{hb}, needs to be small, while the local Rossby number, Ro_b, can be arbitrary. In terms of the core Froude number, F_h, this gives the condition of validity

$$F_h \ll \frac{b^2}{R^2}, \tag{12}$$

meaning that this asymptotic approach is valid for both small and moderate Froude numbers, since b/R is large.

The matching for $1 \ll r \ll 1/k$ between the core solution and far-field solution for $m = 1$ leads to governing equations for the displacements of each vortex. The equations for the displacements of the vortex labelled 1 are:

$$\begin{aligned}\frac{\mathrm{d}\Delta x_1}{\mathrm{d}t} = &-\left(\frac{\Gamma_2}{2\pi b^2} - f_p\right)\Delta y_1 + \frac{\Gamma_2}{2\pi b^2}\Psi\Delta y_2 \\ &- \frac{\Gamma_1}{2\pi R^2}\omega_r\big(F_{h1},\, Ro_1\big)\Delta y_1 + \frac{\Gamma_1}{2\pi R^2}\omega_i\big(F_{h1},\, Ro_1\big)\Delta x_1,\end{aligned} \tag{13}$$

$$\begin{aligned}\frac{\mathrm{d}\Delta y_1}{\mathrm{d}t} = &\underbrace{-\left(\frac{\Gamma_2}{2\pi b^2} + f_p\right)\Delta x_1}_{(a)} + \underbrace{\frac{\Gamma_2}{2\pi b^2}\chi\Delta x_2}_{(b)} \\ &\underbrace{+\frac{\Gamma_1}{2\pi R^2}\omega_r\big(F_{h1},\, Ro_1\big)\Delta x_1 + \frac{\Gamma_1}{2\pi R^2}\omega_i\big(F_{h1},\, Ro_1\big)\Delta y_1}_{(c)}.\end{aligned} \tag{14}$$

The equations for the displacements of the vortex labelled 2 are identical to (13)–(14) after interchanging subscripts 1 and 2. Remarkably, these equations have exactly the same form as those obtained by Crow (1970) in homogeneous fluids. They contain three different physical effects:

(a) The first term corresponds to the external flow in the vicinity of vortex 1. It consists of a straining flow with strain rate $\Gamma_2/(2\pi b^2)$, due to the vortex 2. There is also a uniform rotation at rate $f_p = (\Gamma_1 + \Gamma_2)/(2\pi b^2)$ due to the rotation of the unperturbed vortices around each other.

(b) The second term is the mutual-induction term (i.e., the effect of the perturbation of vortex 2 on vortex 1). This effect depends on the mutual-induction functions χ and ψ, which

describe how the bending perturbation decays outside the vortex core. In a stratified and rotating fluid, they are

$$\chi = \beta b K_1(\beta b) + \beta^2 b^2 K_0(\beta b), \qquad \Psi = \beta b K_1(\beta b), \tag{15}$$

where $\beta = 2k\,|\Omega_b|/N$ and K_0 and K_1 are the modified Bessel functions of the second kind of zero and first order. They differ from those in homogeneous fluids (Crow 1970):

$$\chi = kbK_1(kb), \qquad \Psi = kbK_1(kb) + k^2b^2K_0(kb), \tag{16}$$

because the perturbation outside the vortex core is irrotational in homogeneous fluids, while it has zero potential vorticity in stratified and rotating fluids.

(c) The last term corresponds to the self-induction (i.e., the effect of a vortex on itself when it is curved). The sinusoidally bent vortex rotates at rate $\Gamma_1\omega_r/(2\pi R^2)$ with damping rate $\Gamma_1\omega_i/(2\pi R^2)$, where ω_r and ω_i are the real and imaginary parts of the self-induction function:

$$\omega\big(F_h, Ro\big) = \frac{\beta^2R^2}{2}\left[-\ln\left(\frac{\beta R}{2}\right) + \delta\big(F_h, Ro\big) - \gamma_e\right], \tag{17}$$

where $\gamma_e = 0.5772$ and

$$\delta\big(F_h, Ro\big) = \lim_{\eta_0\to\infty}\int_0^{\eta_0} \xi^3\Omega(\xi)^2\frac{(Ro\Omega(\xi)+1)^2}{1-F_h^2\Omega(\xi)^2}\mathrm{d}\xi - \ln\eta_0. \tag{18}$$

Again, this expression differs from the self-induction function in homogeneous fluids (Crow 1970)

$$\omega = \frac{k^2R^2}{2}\left(\ln\frac{kR}{2} + \gamma_e - D\right), \tag{19}$$

where D is defined in (4).

Therefore, the nature of the fluid enters equations (13)–(14) only through three functions: the mutual-induction functions, ψ, χ, and the self-induction function, ω. The most important difference between stratified-rotating and homogeneous fluids lies in the self-induction function. When $F_h < 1/\Omega_{\max}$, where $\Omega_{\max}$ is the maximum angular velocity, the self-induction is real and positive whatever the Rossby number, Ro, in contrast to homogeneous fluids, for which self-induction is negative. The physical reason for this inversion will be explained in section 2.3.

When $F_h > 1/\Omega_{\max}$, the denominator in the coefficient (18) is singular at the critical radius, r_c, where $\Omega(r_c) = 1/F_h$ (i.e., at the radius where the Brunt–Väisälä frequency is equal to the dimensional angular velocity of the vortex). This singularity is regularized in the presence of viscous and diffusive effects. Just as for classical critical layers, these effects can be taken into account in the inviscid limit by deforming the contour of integration in the upper complex plane to avoid the critical point. The self-induction function, ω, is then complex with a negative imaginary part, meaning that the bending deformations of the vortex are damped. This critical layer is similar to the one observed on a tilted vortex in a stratified fluid (Boulanger *et al* 2007). Vortex alignment in a quasi-geostrophic fluid is also due to a critical layer of the bending mode (Schecter *et al* 2002). However, this critical layer is different since it occurs where the angular velocity is equal to the frequency, $\Omega(r_c) = \omega$. Here, the latter critical layer has no effect because it is located at $r = \infty$ owing to the hypothesis $kR \ll 1$, which implies $\omega = 0$ at the leading order.

This asymptotic approach has an advantage over the vortex filament method in homogeneous fluid because the leading viscous and diffusive effects can also be easily taken into

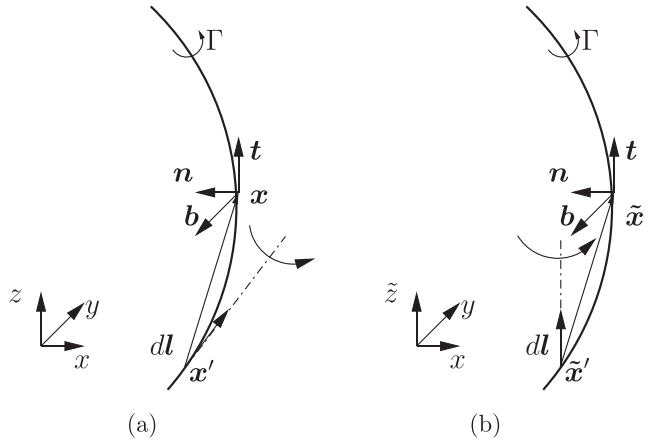

Figure 3. Graphical interpretation of the direction of the self-induced motion of a curved vortex filament in (a) homogeneous fluids and (b) quasi-geostrophic fluids. In (a), the motion induced at $\boldsymbol{x}$ by vortex element $\mathrm{d}\boldsymbol{l}$ is directed in the positive binormal direction, $\boldsymbol{b}$, while in (b), it is directed in the negative binormal direction because the vortex element remains vertical, $\mathrm{d}\boldsymbol{l} = \mathrm{d}l\boldsymbol{e}_z$, even if the vortex is curved. From figure 3 of Billant (2010). © Cambridge University Press, reprinted with permission.

account when there is no critical layer. Only the self-induction function (17) is modified as follows

$$\omega \to \omega - \mathrm{i}\frac{k^2R^2}{Re}\mathcal{V}, \tag{20}$$

where $Re = \Gamma/(2\pi\nu)$ is the Reynolds number and $\mathcal{V}$ is a constant that depends on the angular velocity profile and the Rossby, Froude, and Schmidt numbers (Billant 2010).

2.3. Self-induced motion

The direction of the self-induced motion can be easily explained in cases of homogeneous and quasi-geostrophic fluids. In homogeneous fluids, the Biot–Savart law with the cut off method (2) shows that the self-induced velocity is in the positive binormal direction (figure 3(a)). Hence, it tends to rotate the curved vortex in a direction opposite to the flow in the vortex core.

In the case of a quasi-geostrophic fluid, the potential vorticity and the streamfunction are related by

$$\Pi = \Delta_h\psi + \frac{\partial^2\psi}{\partial\tilde{z}^2}, \tag{21}$$

where $\tilde{z} = (2\,|\Omega_b|/N)z$ is the rescaled vertical coordinate. The velocity field is purely horizontal: $u_x = -\partial\psi/\partial y$ and $u_y = \partial\psi/\partial x$. The relation (21) can be inverted to give a modified Biot–Savart law for a filament of potential vorticity, Π:

$$\boldsymbol{u}(\tilde{\boldsymbol{x}}) = -\frac{\Pi}{4\pi}\int_{|\tilde{\boldsymbol{x}}-\tilde{\boldsymbol{x}}'|>d}\frac{(\tilde{\boldsymbol{x}}-\tilde{\boldsymbol{x}}')\times\mathrm{d}l\boldsymbol{e}_z}{|\tilde{\boldsymbol{x}}-\tilde{\boldsymbol{x}}'|^3} = \frac{\Pi}{4\pi\rho}\boldsymbol{b}\left(\ln\frac{d}{\rho}+O(1)\right), \tag{22}$$

where $\tilde{\boldsymbol{x}} = x\boldsymbol{e}_x + y\boldsymbol{e}_y + \tilde{z}\boldsymbol{e}_z$, d is the cut-off parameter, and ρ is the radius of curvature. The crucial difference is that the vector $\mathrm{d}\boldsymbol{l} = \mathrm{d}l\boldsymbol{e}_z$ always remains vertical, even when the filament is curved, since the motion is constrained to be horizontal (figure 3(b)). As seen in (22), the self-induced motion is in the negative binormal direction, in contrast to (2). Therefore, the curved vortex will spin in the same direction as the flow in the vortex core.

3. Stability analysis of vortex pairs and vortex arrays in a stratified rotating fluid

3.1. Counter-rotating vortex pair

Using equations (13)–(14) and the complementary equations for the second vortex, the stability of a vortex pair can be determined by writing the displacements in the form $(\Delta x_i, \Delta y_i) \propto \exp(\sigma t)$. For the counter-rotating case, $\Gamma_1 = -\Gamma_2 > 0$, considered by Crow (1970), the modes do not separate into two independent classes when Ro is finite like they do in homogeneous fluids. This is because the self-induction of the two vortices are not equal since one vortex is cyclonic and the other is anticyclonic. A separation between symmetric mode ($\Delta x_2 = -\Delta x_1$, $\Delta y_2 = \Delta y_1$) and antisymmetric mode ($\Delta x_2 = \Delta x_1$, $\Delta y_2 = -\Delta y_1$) is recovered only when $Ro \to \infty$ or $Ro \to 0$. Their growth rates are given respectively by

$$\left(\sigma_s - \frac{\Gamma_1}{2\pi R^2}\omega_i\right)^2 = \left(\frac{\Gamma_1}{2\pi b^2}\right)^2\left(1 + \frac{b^2}{R^2}\omega_r + \chi\right)\left(1 - \frac{b^2}{R^2}\omega_r - \Psi\right), \tag{23}$$

$$\left(\sigma_a - \frac{\Gamma_1}{2\pi R^2}\omega_i\right)^2 = \left(\frac{\Gamma_1}{2\pi b^2}\right)^2\left(1 + \frac{b^2}{R^2}\omega_r - \chi\right)\left(1 - \frac{b^2}{R^2}\omega_r + \Psi\right). \tag{24}$$

Since $\Psi = \chi = 1$ and $\omega = 0$ when $k = 0$, both growth rates are zero in the two-dimensional limit: $\sigma_s = \sigma_a = 0$. In this limit, the symmetric mode corresponds to a forward/backward translation of the vortex pair without a change of shape ($\Delta y_2 = \Delta y_1$ with $\Delta x_2 = \Delta x_1 = 0$). Similarly, the antisymmetric mode corresponds to a lateral translation of the whole vortex pair ($\Delta x_2 = \Delta x_1$ with $\Delta y_2 = \Delta y_1 = 0$). These modes are neutral because of the translational invariance in the x- and y-directions. However, when k is no longer zero, they can be destabilized. This can easily be seen by considering the limit $kb \ll 1$. Then, $\Psi \simeq \chi \simeq 1$ at the leading order, and growth rates (23)–(24) can be written as

$$\left(\sigma_s - \frac{\Gamma_1}{2\pi R^2}\omega_i\right)^2 \simeq -2\left(\frac{\Gamma_1}{2\pi b^2}\right)^2\frac{b^2}{R^2}\omega_r, \tag{25}$$

$$\left(\sigma_a - \frac{\Gamma_1}{2\pi R^2}\omega_i\right)^2 \simeq 2\left(\frac{\Gamma_1}{2\pi b^2}\right)^2\frac{b^2}{R^2}\omega_r. \tag{26}$$

We see that either the symmetric mode or the antisymmetric mode is unstable, depending on the sign of the real part of the self-induction function, ω_r. Since ω_r is negative in homogeneous fluids, it is the symmetric mode that is unstable, as found by Crow (1970). In contrast, in strongly stratified fluids, ω_r is positive, so it is the antisymmetric mode which is unstable, in agreement with the observation of the zigzag instability (Billant and Chomaz 2000).

The reason why a negative/positive self-induction destabilizes the symmetric/antisymmetric mode can be simply understood by looking at the full displacement equations for long-wavelength $kb \ll 1$ (i.e., by setting $\Psi = \chi = 1$ in (13)–(14) and the complementary equations). Assuming $\omega_i = 0$ for simplicity, this gives

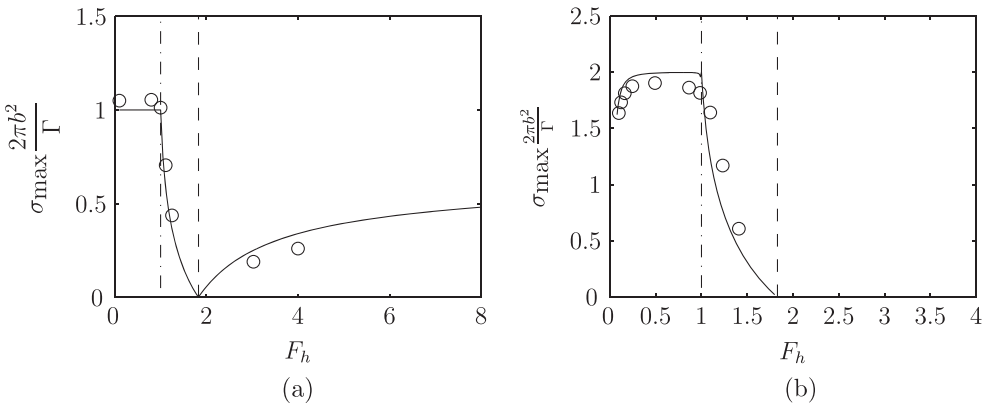

Figure 4. Maximum growth rate as a function of the Froude number for $Ro = \infty$ for (a) counter-rotating vortex pairs with $Re = 50000$, $b/R = 8$, and (b) co-rotating vortex pairs with $Re = 8000$, $b/R = 6.7$. The solid lines show the theoretical prediction, and the symbols show the results of direct numerical stability analyses of pairs of Lamb–Oseen vortices (Otheguy *et al* 2006, Billant *et al* 2010). The dash-dotted line shows the critical Froude number, $F_h = 1$, above which the imaginary part of the self-induction, ω_i, becomes negative. The dashed line indicates the Froude number, $F_h = 1.83$, for which the sign of ω_r changes. Adapted from figures 6(a) and 17(b) of Billant *et al* (2010). © Cambridge University Press, reprinted with permission.

$$\frac{\mathrm{d}\Delta x_1}{\mathrm{d}t} = \frac{\Gamma_1}{2\pi b^2}\left(\Delta y_1 - \Delta y_2\right) - \frac{\Gamma_1}{2\pi R^2}\omega_r \Delta y_1, \tag{27}$$

$$\frac{\mathrm{d}\Delta y_1}{\mathrm{d}t} = \frac{\Gamma_1}{2\pi b^2}\left(\Delta x_1 - \Delta x_2\right) + \frac{\Gamma_1}{2\pi R^2}\omega_r \Delta x_1, \tag{28}$$

$$\frac{\mathrm{d}\Delta x_2}{\mathrm{d}t} = \frac{\Gamma_1}{2\pi b^2}\left(\Delta y_1 - \Delta y_2\right) + \frac{\Gamma_1}{2\pi R^2}\omega_r \Delta y_2, \tag{29}$$

$$\frac{\mathrm{d}\Delta y_2}{\mathrm{d}t} = \frac{\Gamma_1}{2\pi b^2}\left(\Delta x_1 - \Delta x_2\right) - \frac{\Gamma_1}{2\pi R^2}\omega_r \Delta x_2. \tag{30}$$

For the Crow instability, the mode is symmetric, so that $\Delta y_2 = \Delta y_1$. When $\Delta y_1 > 0$, equations (27) and (29) show that Δx_1 increases while Δx_2 decreases when the self-induction, ω_r, is negative. This means that the separation distance between the two vortices decreases, implying that the propagation velocity of the vortex pair increases. Thus, Δy_1 and Δy_2 further increases, as expressed by (28) and (30). For the zigzag instability, the mode is antisymmetric, so that $\Delta x_2 = \Delta x_1$. If $\Delta x_1 > 0$, equations (28) and (30) show that Δy_1 increases while Δy_2 decreases when the self-induction, ω_r, is positive. This means that the vortex pair will turn and propagate slightly obliquely, so that Δx_1 and Δx_2 increase further, as indicated by (27)–(29). If the sign of ω_r is reversed, the feedback is stabilizing in both cases.

In both homogeneous and strongly stratified rotating fluids, the maximum growth rate of these bending instabilities is of the order of the strain, $\Gamma_1/(2\pi b^2)$, and it is reached for a finite vertical wavenumber. The most amplified wavelength is of the order of the separation distance, $\lambda \propto b$, in homogeneous fluids while in strongly stratified fluids, it scales like $\lambda \propto F_h b$ for $Ro \to \infty$ and like $\lambda \propto bF_h/|Ro|$ for $Ro \to 0$.

The effect of the Froude number on the maximum growth rate is displayed in figure 4(a) (Billant *et al* 2010). The maximum growth rate remains constant and equal to unity when $F_h < 1/\Omega_{\max} = 1$, but when F_h is increased above unity, it drops abruptly since the bending modes are damped by the critical layer. The growth rate goes to zero for $F_h = 1.83$ because the real part of the self-induction, ω_r, becomes negative for this critical Froude number. For $F_h > 1.83$, the growth rate rises again slowly when F_h is further increased, but the symmetry of the mode is reversed; it is the symmetric mode that is unstable, like in a homogeneous fluid, since ω_r is negative. The symbols show the results of a numerical stability analysis of two counter-rotating Lamb–Oseen vortices with a separation distance, $b/R = 8$, and for $Re = 50\,000$. The basic vortices were first adapted to each other by means of a two-dimensional simulation. We see that the agreement between the numerical and theoretical results is very good.

3.2. Co-rotating vortex pair

In the case of a co-rotating vortex pair, $\Gamma_1 = \Gamma_2$, the modes always separate into symmetric and antisymmetric modes with growth rate

$$\left(\sigma_s - \frac{\Gamma_1}{2\pi R^2}\omega_i\right)^2 = \left(\frac{\Gamma_1}{2\pi b^2}\right)^2\left(3 - \frac{b^2}{R^2}\omega_r + \chi\right)\left(-1 + \frac{b^2}{R^2}\omega_r + \Psi\right), \tag{31}$$

$$\left(\sigma_a - \frac{\Gamma_1}{2\pi R^2}\omega_i\right)^2 = \left(\frac{\Gamma_1}{2\pi b^2}\right)^2\left(3 - \frac{b^2}{R^2}\omega_r - \chi\right)\left(-1 - \frac{b^2}{R^2}\omega_r - \Psi\right). \tag{32}$$

As before, it is interesting to look first at the long-wavelength limit, $kb \ll 1$, of these equations:

$$\left(\sigma_s - \frac{\Gamma_1}{2\pi R^2}\omega_i\right)^2 \simeq 4\left(\frac{\Gamma_1}{2\pi b^2}\right)^2\frac{b^2}{R^2}\omega_r, \tag{33}$$

$$\left(\sigma_a - \frac{\Gamma_1}{2\pi R^2}\omega_i\right)^2 \simeq -\left(\frac{\Gamma_1}{2\pi b^2}\right)^2\left(4 - \frac{b^4}{R^4}\omega_r^2\right). \tag{34}$$

This shows that the symmetric mode can be unstable in the long-wavelength limit $kb \ll 1$ if ω_r is positive. In contrast, the antisymmetric mode has a nonzero frequency in the two-dimensional limit, and therefore cannot become unstable for small kb. This comes from the fact that two co-rotating vortices rotate around each other, and therefore possess only one invariance in the limit $k = 0$: the rotational invariance from which the symmetric mode originates.

In agreement with these arguments, we see in figure 4(b) that the maximum growth rate is positive when $F_h < 1.83$, and it remains zero when $F_h > 1.83$ (i.e., when ω_r is negative). Just as for counter-rotating vortex pairs, the growth rate is almost constant for $F_h < 1/\Omega_{\max} = 1$ and then drops abruptly because of the critical layers (Otheguy *et al* 2006, 2007, Billant *et al* 2010). There is a slight decrease in the growth rate for small Froude number because the Reynolds number, $Re = 8000$, is not as high as it is in figure 4(a). Viscous and diffusive effects increase when F_h decreases, since the most amplified wavelength scales like F_h.

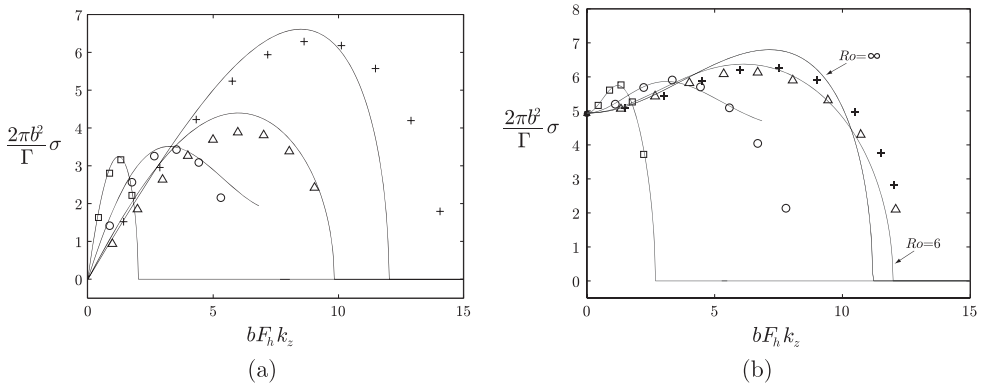

Figure 5. Nondimensional growth rate $2\pi b^2\sigma/\Gamma$ of the dominant mode as a function of the rescaled vertical wavenumber, $bF_h k_z$, for $F_h = 0.1$ for (a) the Kármán vortex street with $\kappa = 0.2$, and (b) the symmetric double row with $\kappa = 0.5$. The symbols correspond to the numerical results for $Re = 50000$, and the solid lines correspond to the asymptotic theory. The symbols correspond to the Rossby numbers $Ro = \infty$ (+), $Ro = 6$ (△), $Ro = 2$ (○), and $Ro = 0.75$ (□). The radius of the vortices is $R = b/15$. From figures 15(a) and 18 of Deloncle *et al* (2011). © Cambridge University Press, reprinted with permission.

3.3. Vortex arrays

This theoretical approach can be easily generalized to study the stability of any number of well-separated vortices (Deloncle *et al* 2011). The only additional complexity is that the mutual-induction and strain effects of all the vortices have to be taken into account. This approach has been used to study the stability of the Kármán vortex street, the symmetric double row, and the single row of co-rotating vortices in stratified-rotating fluid.

These vortex arrays are all unstable in the two-dimensional limit except the Kármán vortex street for the spacing ratio $\kappa \equiv h/b = 0.281$, where h is the distance between the rows and b is the distance between vortices in the same row (Lamb 1932). The three-dimensional stability in homogeneous fluid has been investigated by Robinson and Saffman (1982). The dominant instability for the Kármán vortex street when $\kappa \lesssim 0.3$ is three-dimensional anti-symmetric, with all the vortices of a row being displaced in the same direction. For $\kappa \gtrsim 0.3$, the dominant instability is a two-dimensional pairing instability of adjacent vortices of the same row. In the case of the symmetric double row, the most dangerous instability for any separation ratio, κ, is three-dimensional and symmetric, with displacement in alternating directions every two vortices.

In the case of a stratified-rotating fluid with $F_h < 1/\Omega_{\max} = 1$, the Kármán vortex street is most unstable to a three-dimensional instability, regardless of the Rossby number when $\kappa < 0.4$ (figure 5(a)). The mode is symmetric for $Ro = 0$ and $Ro = \infty$, with all the vortices of a row being displaced in the same direction (figure 6(a)). Hence, there is a reversal of the symmetry of the dominant mode compared to homogeneous fluids, just as there is for counter-rotating vortex pairs. The symmetry of the most unstable mode is also reversed for the symmetric double row for $Ro = 0$ and $Ro = \infty$; it is antisymmetric, with displacement in alternating directions every two vortices (figure 6(b)). Just as for vortex pairs, the maximum growth rate scales like the strain $\Gamma/(2\pi b^2)$, and the most amplified wavelength scales like bF_h for $|Ro| \gg 1$, and like $bF_h/|Ro|$ for $|Ro| \ll 1$. In the case of the single row, the dominant

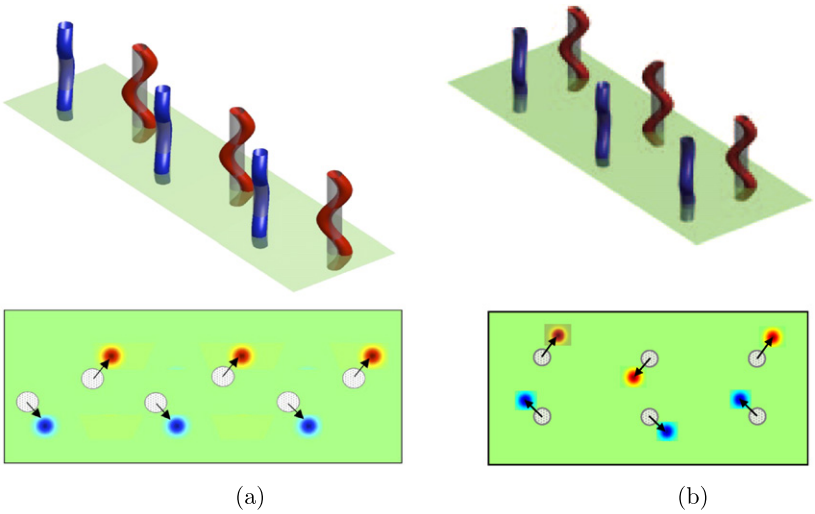

Figure 6. Sketch of the dominant instability of (a) the Kármán vortex street with close rows $\kappa = 0.2$, and (b) the symmetric double row for $\kappa = 0.5$, for $F_h = 0.1$ and $Ro = \infty$. The top figure is a three-dimensional view of the bending deformations induced by the instability. The displacements of the vortices in the horizontal cross section are indicated in the bottom figure. The dominant instability is symmetric, with all the vortices of a row being displaced in the same direction in (a). The dominant instability is antisymmetric, with displacement in alternating direction every two vortices in (b). From Deloncle *et al* (2011).

instability remains a two-dimensional pairing instability. When $F_h > 1$, a critical layer appears and damps these three-dimensional instabilities.

These theoretical results are also in good agreement with numerical stability analyses of vortex arrays made of Lamb–Oseen vortices adapted to each other (figure 5). Moreover, no other types of instability have been found in the numerical stability analyses, proving that bending instabilities are the most dangerous in the range of the vertical wavenumbers investigated. Nevertheless, for larger wavenumbers, short wavelength instabilities might exist, such as the centrifugal instability on anticyclonic vortices.

4. Conclusion

The stability of vortices can be analyzed in stratified-rotating fluids by means of an asymptotic approach that is analogous to vortex filaments in homogeneous fluid. The two main hypotheses are that the vortices are well-separated and perturbed by long-wavelength bending deformations. The results are in good quantitative agreement with numerical stability analyses of vortices with finite cores. The main particularity of strongly stratified-rotating flows is that the self-induced motion of curved vortices is opposite to the one in homogeneous fluids. This explains why the instabilities due to vortex interactions are different in stratified-rotating fluids and homogeneous fluids. Another particularity is that the bending modes are damped by a critical layer when the Froude number is larger than unity. For this reason, the bending instabilities have a reduced growth rate as soon as the Froude number is larger than unity.

Even if only small vortex displacements have been considered, this approach could be generalized to finite displacements. Indeed, the translational invariance implies that if $\psi_1(x, y)$

is a solution of the Euler equations, then $\psi_1(x - \tilde{\Delta}x_1, y - \tilde{\Delta}y_1)$ is also a solution, whatever the amplitude of the displacements $(\tilde{\Delta}x_1, \tilde{\Delta}y_1)$. Three-dimensional effects will be small provided that $\partial\tilde{\Delta}x_1/\partial z \ll 1$ and $\partial\tilde{\Delta}y_1/\partial z \ll 1$. Hence, an asymptotic analysis could be conducted, provided that the displacements vary weakly with z, but their amplitudes can be finite. Similarly, this approach is not limited to columnar vortices, but can also be applied to baroclinic vortices, $\psi_1(x, y, z)$. The translational invariance indeed remains valid, implying that $\psi_1(x - \tilde{\Delta}x_1, y - \tilde{\Delta}y_1, z)$ is a solution regardless of the displacements $(\tilde{\Delta}x_1, \tilde{\Delta}y_1)$. Hence, this approach could be extended to study the non-linear evolution of bending instabilities and their development for baroclinic vortices. This will be considered in the future.

Acknowledgments

We thank Y Fukumoto and all the members of the organizing committee of the IUTAM Symposium for the opportunity to present this work.

References

Billant P 2010 Zigzag instability of vortex pairs in stratified and rotating fluids: I. General stability equations *J. Fluid Mech.* **660** 354–95

Billant P and Chomaz J M 2000 Experimental evidence for a new instability of a vertical columnar vortex pair in a strongly stratified fluid *J. Fluid Mech.* **418** 167–88

Billant P, Deloncle A, Chomaz J M and Otheguy P 2010 Zigzag instability of vortex pairs in stratified and rotating fluids: II. Analytical and numerical analyses *J. Fluid Mech.* **660** 396–429

Billant P and Gallaire F 2005 Generalized Rayleigh criterion for non-axisymmetric centrifugal instabilities *J. Fluid Mech.* **542** 365–79

Boulanger N, Meunier P and le Dizès S 2007 Structure of a tilted stratified vortex *J. Fluid Mech* **583** 443–58

Crow S C 1970 Stability theory for a pair of trailing vortices *AIAA J.* **8** 2172–9

Deloncle A, Billant P and Chomaz J M 2011 Three-dimensional stability of vortex arrays in a stratified and rotating fluid: theoretical analysis *J. Fluid Mech.* **678** 482–510

Dritschel D G and de la Torre Juárez M 1996 The instability and breakdown of tall columnar vortices in a quasi-geostrophic fluid *J. Fluid Mech.* **328** 129–60

Fukumoto Y and Miyazaki T 1991 Three-dimensional distortions of a vortex filament with axial velocity *J. Fluid Mech.* **222** 369–416

Jiménez J 1975 Stability of a pair of co-rotating vortices *Phys. Fluids* **18** 1580–1

Kerswell R R 2002 Elliptical instability *Annu. Rev. Fluid Mech.* **34** 83–113

Kloosterziel R C and van Heijst G J F 1991 An experimental study of unstable barotropic vortices in a rotating fluid *J. Fluid Mech.* **223** 1–24

Lamb H 1932 *Hydrodynamics* (Cambridge: Cambridge University Press)

Leblanc S 2003 Internal wave resonances in strain flows *J. Fluid Mech.* **477** 259–83

Leibovich S, Brown S N and Patel Y 1986 Bending waves on inviscid columnar vortices *J. Fluid Mech.* **173** 595–624

Miyazaki T 1993 Elliptical instability in a stably stratified rotating fluid *Phys. Fluids* A **5** 2702–9

Miyazaki T and Fukumoto Y 1992 Three-dimensional instability of strained vortices in stably stratified fluid *Phys. Fluids* A **4** 2515–22

Moore D W and Saffman P G 1972 Motion of a vortex filament with axial-flow *Phil. Trans. R. Soc.* A **272** 403–29

Otheguy P 2005 *PhD Thesis* Ecole Polytechnique

Otheguy P, Billant P and Chomaz J M 2006 The effect of planetary rotation on the zigzag instability of co-rotating vortices in a stratified fluid *J. Fluid Mech.* **553** 273–81

Otheguy P, Billant P and Chomaz J M 2007 Theoretical analysis of the zigzag instability of a vertical co-rotating vortex pair in a strongly stratified fluid *J. Fluid Mech.* **584** 103–23

Otheguy P, Chomaz J M and Billant P 2006 Elliptic and zigzag instabilities on co-rotating vertical vortices in a stratified fluid *J. Fluid Mech.* **553** 253–72

Riley J J and Lelong M P 2000 Fluid motions in the presence of strong stable stratification *Annu. Rev. Fluid Mech.* **32** 617–57

Robinson A C and Saffman P G 1982 Three-dimensional stability of vortex arrays *J. Fluid Mech.* **125** 411–27

Saffman P G 1992 *Vortex Dynamics* (Cambridge: Cambridge University Press)

Schecter D A, Montgomery M T and Reasor P D 2002 A theory for the vertical alignment of a quasigeostrophic vortex *J. Atmos. Sci.* **59** 150–68

Widnall S E, Bliss D and Zalay A 1971 Theoretical and experimental study of the stability of a vortex pair *Proc. Symp. on Aircraft, Wake Turbulence (Seattle)* ed J H Olsen, A Goldburg and M Rogers (New York: Plenum) p 305